

TRACKING QUINTESSENCE, WIMP RELIC DENSITY, PAMELA AND FERMI LAT

C. PALLIS

Department of Physics, University of Patras, GR-265 00 Patras, GREECE

The generation of an early *kination dominated* (KD) era within a tracking quintessential model is investigated, the relic density of the *Weakly Interacting Massive Particles* (WIMPs) is calculated and we show that it can be enhanced *with respect to* (w.r.t) its value in the *Standard Cosmology* (SC). By adjusting the parameters of the quintessential scenario, the cold dark matter abundance in the universe can become compatible with large values for the annihilation cross section times the velocity of the WIMPs. Using these values and assuming that the WIMPs annihilate predominantly to $\mu^+\mu^-$, we calculate the induced fluxes of e^\pm cosmic rays and fit the current PAMELA and Fermi-LAT data. We achieve rather good fits in conjunction with a marginal fulfillment of the restriction arisen from the *Cosmic Microwave Background* (CMB).

1 INTRODUCTION

A plethora of recent data [1] indicates that the two major components of the universe are the *Cold Dark Matter* (CDM) and *Dark Energy* (DE). The DE component can be explained with the introduction of a slowly evolving today scalar field, q , called quintessence whereas WIMPs, χ , are the most natural candidates to account for CDM. In this talk, which is based on Ref. [2], we reconsider (Sec. 2) the creation of an early era dominated by the kinetic energy of q in the context of a tracking quintessential model [3]. We show (Sec. 3) that if χ decouples from the cosmic fluid during this era, its relic abundance, $\Omega_\chi h^2$ can be significantly enhanced w.r.t. its value in SC. This enhancement of $\Omega_\chi h^2$ assists us to interpret, through the χ 's annihilation in the galaxy (Sec. 4), the reported [4, 5] excess on the positron (e^+) and/or electron (e^-) *cosmic-ray* (CR) flux under the assumption that χ 's annihilate predominantly into $\mu^+\mu^-$ (Sec. 5). Throughout, the subscript 0 [I] is referred to present-day values [to values at the onset of our scenario] and $\bar{\rho}_i = \rho_i/\rho_{c0}$ ($i = q, R$ and M) where $\rho_{c0} = 8.1 \cdot 10^{-47} h^2 \text{ GeV}^4$ with $h = 0.72$.

2 THE TRACKING QUINTESSENTIAL MODEL

The quintessence field, q , of our *quintessential scenario* (QS) satisfies the equation:

$$\ddot{q} + 3H\dot{q} + dV/dq = 0, \text{ with } V = M^{4+a}/q^a + bH^2q^2/2 \text{ and } H/H_0 = \bar{H} = \sqrt{\bar{\rho}_q + \bar{\rho}_R + \bar{\rho}_M}. \quad (1)$$

Here H is the Hubble parameter, dot denotes derivative w.r.t the cosmic time t , $\rho_q = \dot{q}^2/2 + V$, $\rho_R \simeq \rho_{R0} \exp(-4\tau)$ and $\rho_M = \rho_{M0} \exp(-3\tau)$ is the q , radiation and matter energy density respectively, $\tau = \ln(R/R_0)$ is the logarithmic time and R is the scale factor of the universe.

We impose on our QS the following constraints:

- Initial Domination of Kination.* We focus our attention in the range of parameters with $\Omega_{qI} = \Omega_q(\tau_I) = 1$ where $\Omega_q \simeq \rho_q/(\rho_q + \rho_R + \rho_M)$ is the quintessential energy-density parameter.
- Inflationary Constraint.* Assuming that the power spectrum of the curvature perturbations is generated by an early inflationary stage, we impose the bound $\bar{H}_I \lesssim 1.72 \cdot 10^{56}$.
- Nucleosynthesis (BBN) Constraint.* At the onset of BBN, $\tau_{\text{BBN}} = -22.3$, ρ_q is to be sufficiently suppressed compared to ρ_R , i.e., [6] $\Omega_q(\tau_{\text{BBN}}) \leq 0.21$ at 95% confidence level (c.l.).

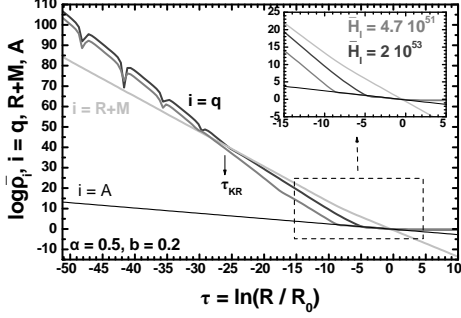


FIG. 1 The evolution of $\log \bar{\rho}_i$ with $i = q$ (gray [dark gray] line), $R+M$ (light gray line) and A (thick line) as a function of τ for $\bar{q}_1 = 0.01$, $a = 0.5$, $b = 0.2$, $T_I = 10^9$ GeV, $M = 4.8$ eV and $\bar{H}_I = 4.7 \cdot 10^{51}$ [$\bar{H}_I = 2 \cdot 10^{53}$] – note that $\bar{\rho}_{R+M} = \bar{\rho}_R + \bar{\rho}_M$. We observe that although the used \bar{H}_I 's differ by two orders of magnitude, both $\bar{\rho}_q$'s reach $\bar{\rho}_A$ highlighting thereby the insensitivity of our QS to the initial conditions.

- (d) *DE and Cosmic Coincidence Constraint.* These two requirements can be addressed if we demand [3] $\Omega_{q0} = \bar{\rho}_{q0} = 0.74$ and $d^2V(\tau = 0)/dq^2 \simeq H_0^2$.
- (e) *Acceleration Constraint.* Successful quintessence has to account for the present-day acceleration of the universe, i.e. [1] $-1.12 \leq w_q(0) \leq -0.86$ (95% c.l.), where $w_q = (\dot{q}^2/2 - V)/(\dot{q}^2/2 + V)$ is the barotropic index of the q -field.

Solving Eq. (1) we find that q undergoes four phases during its evolution – see Fig. 1. For $\tau < \tau_{KR}$ the universe and q is dominated by $\dot{q}/2 \gg V$ and therefore we get a KD era, during which q is set in anharmonic oscillations for $b > 0$. In particular, \bar{q} develops extrema at

$$\tau_{\text{ext}} \simeq (2k + 1) \sqrt{\frac{1}{b} \frac{\pi}{2}} + \tau_I, \text{ with } k = 0, 1, 2, \dots \quad (2)$$

For $\tau > \tau_{KR}$ the universe becomes initially radiation and then matter dominated whereas ρ_q is dominated initially by $\dot{q}/2$ and then by V . As τ approaches 0 the system in Eq. (1) admits [3] a tracking solution since the energy density of the attractor:

$$\bar{\rho}_A \propto \exp(-3(1 + w_q^{\text{fp}})\tau) \text{ with } w_q^{\text{fp}} = -2/(a + 2) \quad (3)$$

tracks $\bar{\rho}_M$ until it outstrips and dominates the current expansion of the universe. It can be shown [2,3] that $b > 0$ ensures the coexistence of an early KD phase with the achievement of the tracking solution in time. Moreover, for $a < 0.6$ the requirement 2-(e) can be marginally fulfilled, too.

3 THE WIMP RELIC DENSITY

The relic density of a WIMP χ , $\Omega_\chi h^2$, with mass m_χ is calculated using the formula:

$$\Omega_\chi h^2 = 2.748 \cdot 10^8 (n_{\chi 0}/s_0) (m_\chi/\text{GeV}), \text{ where } \dot{n}_\chi + 3Hn_\chi + \langle \sigma v \rangle (n_\chi^2 - n_\chi^{\text{eq}2}) = 0 \quad (4)$$

is the Boltzmann equation which governs the evolution of the χ 's number density, n_χ . Also, $n_\chi^{\text{eq}} \propto x^{3/2} e^{-1/x}$ with $x = T/m_\chi$ is the equilibrium configuration of n_χ , $\langle \sigma v \rangle$ is the thermal-averaged cross section times the velocity of χ 's and $s \propto T^3$ is the entropy density with T the temperature.

The decoupling of χ from the cosmic fluid during the QS and SC is visualized in Fig. 2-(a). We observe that, in both cases, the current ρ_χ/s follows ρ_χ^{eq}/s and at some $\tau = \tau_F$, ρ_χ/s dominates over ρ_χ^{eq}/s and remains constant until today. For the selected m_χ and $\langle \sigma v \rangle$ we obtain an enhancement of $\Omega_\chi h^2$ within QS w.r.t its value in the SC, $\Omega_\chi h^2|_{\text{QS}}$, since $\Omega_\chi h^2 = 0.11$ whereas $\Omega_\chi h^2|_{\text{SC}} = 0.0045$. This enhancement can be further analyzed, by defining $\Delta\Omega_\chi = \Omega_\chi h^2 / \Omega_\chi h^2|_{\text{SC}} - 1$. The behavior of $\Delta\Omega_\chi$ as a function of the free parameters of the QS can be inferred from Fig. 2-(b). For $b = 0$ we obtain a pure KD era and $\Delta\Omega_\chi$ increases when m_χ increases or $\langle \sigma v \rangle$ decreases. For $b \neq 0$, $\Delta\Omega_\chi$ depends crucially on the hierarchy between τ_F and τ_{ext} . As m_χ increases above 0.1 TeV, τ_F decreases and moves closer to τ_{ext} and $\Delta\Omega_\chi$ decreases with its minimum $\Delta\Omega_\chi|_{\text{min}}$ occurring at $m_\chi = m_\chi|_{\text{min}}$ which corresponds to $\tau_F^{\text{min}} \simeq \tau_{\text{ext}}$.

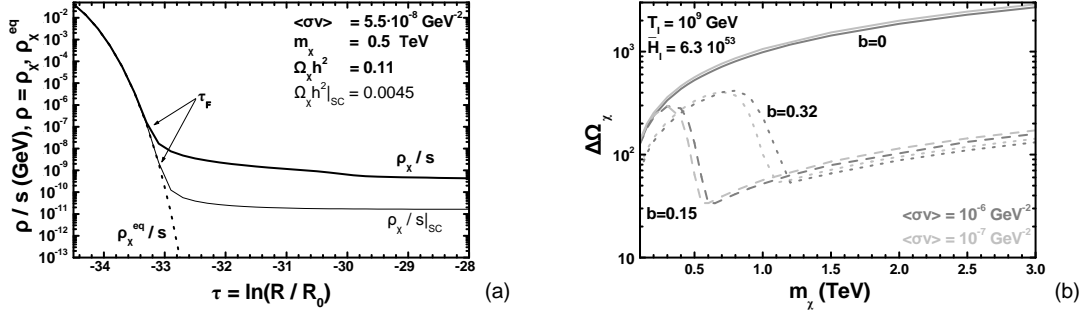


FIG. 2 (a) The evolution as a function of τ of the quantities $\rho_\chi^{\text{eq}}/s = m_\chi n_\chi^{\text{eq}}/s$ (dotted line) and $\rho_\chi/s = m_\chi n_\chi/s$ (thick [thin] solid lines) for the QS [SC]; (b) $\Delta\Omega_\chi$ versus m_χ for the QS with $a = 0.5$, $\bar{H}_1 = 6.3 \cdot 10^{53}$, $T_1 = 10^9 \text{ GeV}$, $\langle\sigma v\rangle = 10^{-6} \text{ GeV}^{-2}$ [$\langle\sigma v\rangle = 10^{-7} \text{ GeV}^{-2}$] (gray [light gray] lines) and $b = 0$ (solid lines), $b = 0.15$ (dashed lines) and $b = 0.32$ (dotted lines).

4 e^\pm -CRS FROM WIMP ANNIHILATION

Residual χ 's annihilations in the galaxy induce a e^+ flux per energy at Earth which is given by

$$\Phi_{e^+}^{\chi\chi}(E) = \frac{1}{2} \frac{v_{e^+}}{4\pi b(E)} \left(\frac{\rho_\odot}{m_\chi} \right)^2 \langle\sigma v\rangle \int_E^{m_\chi} dE' I(\lambda_D(E, E')) \frac{dN_{e^+}}{dE'} , \quad \text{where} \quad (5)$$

v_{e^+} is the velocity of e^+ , $\rho_\odot = 0.3 \text{ GeV/cm}^3$ is the local CDM density, $b(E) = E^2/(\text{GeV} t_E)$ with $t_E = 10^{16} \text{ s}$ is the energy loss rate function and dN_{e^+}/dE_{e^+} denotes the energy distribution of e^+ 's per χ annihilation and can be found in Ref. [7]. Also, $I(\lambda_D)$ is the dimensionless halo function which fully encodes the galactic astrophysics and can be read off from Ref. [8]

There are three sources of uncertainty in our computation: the CDM distribution, the propagation of χ annihilation products and the astrophysical backgrounds. We adopt (a) the isothermal halo profile, to avoid troubles with observations on γ -CRs; (b) the MED propagation model, which provides the best fits to the combinations of the two data-sets; and (c) commonly [8] assumed background e^\pm fluxes normalized with the Fermi-LAT data. Adding the latter contributions to the one in Eq. (5) we get the total fluxes, Φ_{e^\pm} .

In order to qualify our fittings to the experimental data, we define the χ^2 variables as follows:

$$\chi_A^2 = \sum_{i=1}^{N_A} \frac{(F_{Ai}^{\text{obs}} - F_{Ai}^{\text{th}})^2}{(\Delta F_{Ai}^{\text{obs}})^2}, \quad \text{with } F_A = \begin{cases} \Phi_{e^+}/(\Phi_{e^+} + \Phi_{e^-}) & \text{and } N_A = 7 \text{ for PAMELA,} \\ E_{e^+}^3/(\Phi_{e^+} + \Phi_{e^-}) & \text{and } N_A = 26 \text{ for Fermi LAT,} \end{cases} \quad (6)$$

where i runs over the data points of each experiment A , ‘‘obs’’ [‘‘th’’] stands for measured [theoretically predicted] values. The best fits to the combined experimental data can be achieved with $m_\chi \simeq 1.28 \text{ TeV}$ and $\langle\sigma v\rangle \simeq 1.95 \cdot 10^{-6} \text{ GeV}^{-2}$ resulting to $(\chi_1^2 + \chi_2^2)/\text{d.o.f} = 24/31$.

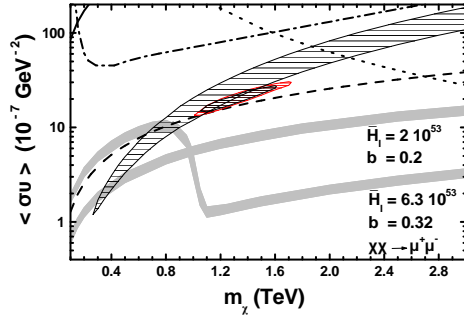
5 RESULTS

To systematize our approach, we can define regions in the $m_\chi - \langle\sigma v\rangle$ plane which are favored at 95% c.l. [99% c.l.] by the various experimental data on the e^\pm -CRs demanding

$$\chi^2 \lesssim \chi^2|_{\text{min}} + 6 \left[\chi^2 \lesssim \chi^2|_{\text{min}} + 9.2 \right] \quad \text{with } \chi^2 = \begin{cases} \chi_1^2 & \text{for PAMELA,} \\ \chi_1^2 + \chi_2^2 & \text{for PAMELA and Fermi LAT,} \end{cases}$$

where $\chi^2|_{\text{min}}$ can be extracted numerically by minimization of χ^2 w.r.t m_χ and $\langle\sigma v\rangle$.

The large $\langle\sigma v\rangle$'s which are required in order to fit the experimental data on e^\pm -CRs are to be consistent with a number of requirements so as the interpretation of the data on e^\pm -CRs via CDM annihilation in the galaxy is fully acceptable. All in all, we impose the following constraints:



m_χ	1.12 TeV		
$\langle\sigma v\rangle$	$1.44 \cdot 10^{-6} \text{ GeV}^{-2}$		
$\Omega_\chi h^2 _{\text{SC}}$	0.00019		
PARAMETERS YIELDING $\Omega_\chi h^2 = 0.11$			
IN OUR QS ($a = 0.5$, $T_I = 10^9 \text{ GeV}$)			
b	0	0.08	0.18
$\bar{H}_I/10^{53}$	3.1	3.4	4.7
$T_{\text{KR}} \text{ (GeV)}$	0.019	0.005	0.009

FIG. 3 Restrictions in the $m_\chi - \langle\sigma v\rangle$ plane for $a = 0.5$, $T_I = 10^9 \text{ GeV}$ and several b 's and \bar{H}_I 's indicated in the graph. The light gray shaded areas are allowed the constraint 5-(a), the sparse black hatched area is preferred at 95% c.l. by the PAMELA data and the dense black [red] hatched areas are preferred at 95% c.l. [99% c.l.] by the PAMELA and Fermi-LAT data. Regions above the black solid, dashed, dot-dashed and dotted lines are ruled out by the upper bounds on $\langle\sigma v\rangle$ from the constraints 5-(b), 5-(c) 5-(d) and 5-(e), respectively. The best-fit $(m_\chi, \langle\sigma v\rangle)$ for the combination of PAMELA and Fermi-LAT data which is consistent with all the constraints is given in the table. Shown are also $\Omega_\chi h^2|_{\text{SC}}$ and several b 's and \bar{H}_I 's (and the resulting T_{KR} 's) leading to $\Omega_\chi h^2 \simeq 0.11$ in our QS.

- (a) Constraint from the CDM abundance [1]: $0.097 \lesssim \Omega_\chi h^2 \lesssim 0.12$.
- (b) BBN constraint [9]: $\langle\sigma v\rangle \leq 8.6 \cdot 10^{-5} \text{ GeV}^{-2} (m_\chi/\text{TeV})$.
- (c) CMB constraint [10]: $\langle\sigma v\rangle \leq 1.3 \cdot 10^{-6} \text{ GeV}^{-2} (m_\chi/\text{TeV})$.
- (d) Constraint from the γ -CRs [11]: $\langle\sigma v\rangle \lesssim 4 \cdot 10^{-6} \text{ GeV}^{-2}$ for the isothermal halo profile.
- (e) Unitarity constraint: $\langle\sigma v\rangle \leq 8\pi \text{ GeV}^{-2} (m_\chi/\text{GeV})^{-2}$.

Imposing all the constraints above we can delineate our findings in the $m_\chi - \langle\sigma v\rangle$ plane as in Fig. 3. A simultaneous interpretation of the e^\pm -CR anomalies consistently with the various constraints can be achieved in the regions where the gray shaded areas overlap the lined ones below the dashed lines. We observe that part of the region favored at 99% c.l. by PAMELA and Fermi LAT is allowed. The best-fit $(m_\chi, \langle\sigma v\rangle)$ – with $\chi^2/\text{d.o.f} = 33/31$ – which saturates the most stringent (CMB) bound is arranged in the Table of Fig. 3. We remark that the requirement 5-(a) is violated within SC but can be met by adjusting the parameters of the QKS. In all cases we obtain $T_{\text{KR}} < 0.02 \text{ GeV}$ with T_{KR} being the transition temperature to the conventional RD era. It remains the construction of a particle model with the appropriate couplings so that χ 's annihilate into $\mu^+\mu^-$ with the desired $\langle\sigma v\rangle$ derived self-consistently with the (s)particle spectrum.

Acknowledgements This research was funded by the FP6 Marie Curie Excellence grant MEXT-CT-2004-014297.

REFERENCES

- [1] E. Komatsu *et al.* [WMAP Collaboration], *Astrophys. J. Suppl.* **180**, 330 (2009).
- [2] S. Lola, C. Pallis and E. Tzelati, *J. Cosmol. Astropart. Phys.* **11**, 017 (2009); C. Pallis, [arXiv:0909.3026](https://arxiv.org/abs/0909.3026) (to appear in *Nucl. Phys.* **B**).
- [3] A. Masiero, M. Pietroni and F. Rosati, *Phys. Rev. D* **61**, 023504 (2000); F. Rosati, *Phys. Lett. B* **570**, 5 (2003).
- [4] O. Adriani *et al.* [PAMELA Collaboration], *Nature* **458**, 607 (2009).
- [5] A.A. Abdo *et al.* [The Fermi-LAT Collaboration], *Phys. Rev. Lett.* **102**, 181101 (2009).
- [6] R.H. Cyburt *et al.*, *Astropart. Phys.* **23**, 313 (2005).
- [7] I.Z. Rothstein, T. Schwetz and J. Zupan, *J. Cosmol. Astropart. Phys.* **07**, 018 (2009).
- [8] E.A. Baltz and J. Edsjo, *Phys. Rev. D* **59**, 023511 (1999); T. Delahaye *et al.*, *Phys. Rev. D* **77**, 063527 (2008); M. Cirelli, R. Franceschini and A. Strumia, *Nucl. Phys.* **B800**, 204 (2008).
- [9] J. Hisano, M. Kawasaki, K. Kohri, T. Moroi and K. Nakayama, *Phys. Rev. D* **79**, 083522 (2009).
- [10] T.R. Slatyer, N. Padmanabhan and D.P. Finkbeiner, *Phys. Rev. D* **80**, 043526 (2009).
- [11] G. Bertone, M. Cirelli, A. Strumia and M. Taoso, *J. Cosmol. Astropart. Phys.* **03**, 009 (2009).